The Low Lysine Content of Ricin A Chain Reduces the Risk of Proteolytic Degradation after Translocation from the Endoplasmic Reticulum to the Cytosol†

Emma D. Deeks, Jonathan P. Cook, Philip J. Day, Daniel C. Smith, Lynne M. Roberts, and J. Michael Lord*

Department of Biological Sciences, University of Warwick, Coventry CV4 7AL, U.K.

Received July 30, 2001; Revised Manuscript Received December 20, 2001

ABSTRACT: Several protein toxins, including the A chain of ricin (RTA), enter mammalian cells by endocytosis and subsequently reach their cytosolic substrates by translocation across the endoplasmic reticulum (ER) membrane. To achieve this export, such toxins exploit the ER-associated protein degradation (ERAD) pathway but must escape, at least in part, the normal degradative fate of ERAD substrates. Toxins that translocate from the ER have an unusually low lysine content. Since lysyl residues are potential ubiquitination sites, it has been proposed that this paucity of lysines reduces the chance of ubiquitination and subsequent ubiquitin-mediated proteasomal degradation [Hazes, B., and Read, R. J. (1997) *Biochemistry 36*, 11051−11054]. Here we provide experimental support for this hypothesis. The two lysyl residues within RTA were changed to arginyl residues. Their replacement in RTA did not have a significant stabilizing effect, suggesting that the endogenous lysyl residues are not the usual sites for ubiquitin attachment. However, when four additional lysines were introduced into RTA in a way that did not compromise the activity, structure, or stability of the toxin, degradation was significantly enhanced. Enhanced degradation resulted from ubiquitination that predisposed the toxin to proteasomal degradation. Treatment with the proteasome inhibitor *clasto*-lactacystin β-lactone increased the cytotoxicity of the lysine-rich RTA to a level approaching that of wild-type ricin. The introduction of four additional lysyl residues into a second ribosome-inactivating protein, abrin A chain, also dramatically decreased the cytotoxicity of the holotoxin compared to wild-type abrin. This effect could also be reversed by proteasomal inhibition. Our data support the hypothesis that the evolution of a low lysine content is a degradation-avoidance strategy for toxins that retrotranslocate from the ER.

Ricin is a plant protein that is potently toxic to mammalian cells because it irreversibly inhibits protein biosynthesis (*1*). This results from the catalytic removal of a specific adenine residue from a highly conserved loop in 28S ribosomal RNA (A_{4324} in the case of rat liver) (*2*). Ribosomes containing ricin-modified 28S rRNA are unable to bind elongation factors and, as a consequence, can no longer synthesize protein.

Structurally, ricin is a heterodimer in which the catalytically active polypeptide (the A chain or RTA)[1] is covalently joined by a disulfide bond to a second polypeptide (the B chain or RTB). RTB is a galactose-specific lectin that facilitates toxin binding to the surface of cells by interacting with terminal galactose residues present on surface glycoproteins or glycolipids. Surface-bound ricin enters cells by endocytosis. The productive intracellular trafficking route that results in a toxic effect involves a small proportion of the endocytosed toxin reaching the endoplasmic reticulum (ER), from where reduced RTA is translocated into the cytosol (*3*−*6*).

Export of the reduced toxin polypeptides to the cytosol is a poorly understood process, but evidence is accumulating from both in vivo and in vitro studies to support the contention that protein translocation from the ER involves the Sec61p translocons (*5*, *7*). This conduit permits not only the import of nascent polypeptides but also the export of misfolded or orphan proteins for cytosolic degradation by the proteasome (*8*−*10*). Some native proteins can also be dislocated to the cytosol as part of their cellular regulation [e.g., HMG CoA-reductase (*11*)] or as a result of viral gene expression (*12*). It is therefore plausible that toxins entering the ER upon endocytosis are able to hijack the ER quality control system that normally serves to perceive and target such proteins to the Sec61p channels. The reverse translocation of aberrant proteins to the cytosol is a process that is normally tightly coupled to their cytosolic deglycosylation, ubiquitination, and proteasomal degradation. This overall process is known as ER-associated protein degradation (ERAD) (*10*, *13*).

The most downstream event of the ERAD pathway is proteolysis. This usually involves the ubiquitin/proteasome system that is also critical for the degradation of cytosolic and nuclear proteins (*14*), although there are a few examples of ubiquitin-independent proteasomal degradation (*15*−*17*). Ubiquitin is a highly conserved 76-residue polypeptide

† Supported by a Wellcome Trust Program Grant to L.M.R. and J.M.L.

* To whom correspondence should be addressed. Phone: (44) 2476 523598. Fax: (44) 2476 523701. E-mail: mlord@bio.warwick.ac.uk.

[1] Abbreviations: RTA, ricin A chain; RTB, ricin B chain; ER, endoplasmic reticulum; ERAD, ER-associated protein degradation; ATA, abrin A chain; SDS−PAGE, sodium dodecyl sulfate−polyacrylamide gel electrophoresis; DMEM, Dulbecco's modified Eagle medium; FCS, fetal calf serum; PBS, phosphate-buffered saline; CHO, Chinese hamster ovary; CD, circular dichroism; PAP, pokeweed antiviral protein; RIP, ribosome-inactivating protein.

10.1021/bi011580v CCC: $22.00
Published on Web 02/14/2002

expressed in all eukaryotic cells. The first step in the degradation of proteins by the proteasomes classically involves the sequential, covalent linkage of multiple ubiquitin molecules to target protein lysine(s) or sometimes to the amino terminus of the target (*18*). This process involves the activation of ubiquitin by a specific activating enzyme (E1) followed by its transfer to a ubiquitin carrier protein (E2). Activated ubiquitin is then linked to the target lysine either directly or with the help of an ubiquitin ligase (E3). Although multiple E2 and E3 enzymes exist, there is thought to be only one E1 enzyme. The ubiquitinated protein is then degraded by the 26S proteasomes (reviewed in ref *19*).

Although posing as ERAD substrates provides an appealing explanation as to how toxins might mechanistically achieve export from the ER to the cytosol, to have a physiological effect at least a proportion of the exported toxin must avoid subsequent proteasomal degradation. This conundrum is made all the more tricky in that ubiquitination (*20*) and proteolysis (*21*) can be very tightly coupled to the membrane translocation process. Interestingly, it has been noted that the A chains of toxins translocating from the ER have an unusually low lysine content (*22*). In contrast, the lysine content of their corresponding cell-binding B chains, or of the A chains of toxins known to enter the cytosol from acidified endosomes (for example, the diphtheria toxin A fragment), is much more typical. This observation led to the proposal that the paucity of lysines permitted at least a fraction of toxin to escape the fate of ubiquitin-mediated proteolytic degradation (*22*). Here we provide experimental evidence that this may well be the case.

MATERIALS AND METHODS

Materials. [^{35}S]Methionine was from Amersham, *clasto*-lactacystin β-lactone was from Calbiochem, and ricin B chain was from Vector laboratories. Abrin holotoxin was provided by Dr. E. Wawrzynczak (Institute for Cancer Research, Sutton, U.K.). Ribophorin 1 antibodies and E36 and ts20 CHO cells were a kind gift from Dr. N. E. Ivessa (Department of Molecular Genetics, University and Biocenter Vienna, Vienna, Austria). Trypsin (TPCK-treated, bovine pancreas type XIII) was from Sigma.

Creation of Ricin A Chain Variants. Ricin A chain mutants encoding single or multiple amino acid substitutions were generated by PCR mutagenesis and standard recombinant DNA techniques. Using the RTA expression plasmid pUTA (*23*) as a PCR template, appropriate base changes were introduced (individually) to encode for the single amino acid substitutions V38K, N132K, and S228K. The E67K mutation was generated using the pUTA-RTA(V38K) construct as a template for PCR mutagenesis. The single mutations were then each reintroduced into pUTA to create RTA-V38K/E67K (using *Eco*RI/*Nsi*I), RTA-N132K/S228K (using *Cla*I/*Bgl*II and *Bgl*II/*Pst*I), and RTA-V38K/E67K/N132K/S228K. The pUTA RTA-4R construct was created using exactly the same approach.

Expression and Purification of Ricin A Chain Variants. A 50 mL culture of plasmid-bearing *Escherichia coli* TG2 was grown overnight at 37 °C. This starter culture was used to inoculate 500 mL of 2YT media and the culture grown for 2 h at 30 °C. RTA expression was induced by addition of isopropyl 1-thio-β-D-galactoside (IPTG) to a final concentration of 1 mM for 4 h at 30 °C. Cells were harvested by centrifugation at 5000 rpm, resuspended in 15 mL of 5 mM sodium phosphate buffer, pH 6.5, and broken by sonication. Cell debris was removed by centrifugation at 15000 rpm for 30 min at 4 °C and the RTA-containing supernatant loaded onto a carboxymethyl-Sepharose CL-6B (Pharmacia) column equilibrated in the same buffer. The column was washed with 1000 mL of buffer, followed by 100 mL of buffer containing 100 mM sodium chloride to remove unbound proteins. RTA was eluted with a 500 mL NaCl gradient (100−300 mM). Fractions containing pure RTA were identified by SDS−PAGE, pooled, and stored at 4 °C.

Cloning of the Abrin A Chain Gene. A 5 mm piece of *Abrus precatorius* leaf was boiled with 40 μL of 0.25 M NaOH for 30 s. Forty microliters of 0.25 M HCl plus 20 μL of 0.5 M Tris-HCl, pH 8.0, and 0.25% Triton X-100 was then added. This was boiled for a further 2 min and centrifuged in a microfuge at full speed for 5 min. The pellet was used in the following PCR reaction (5′ primer: GC-GAATTC ATG CAA GAT CAA GTT ATT AAA TTC ACT ACT GAA GGA GCA ACT AGT CAA TCT TAT AAA CAA TTT ATT GAA GCG CTT CGA GAG AG; this primer has modified codon usage to alleviate a possible loop structure which may inhibit protein synthesis. 3′ primer: CGGGATCC TTA ATT TGG CGG ATT GCA GAC AAA AAG). A reaction mixture containing the above primers at 1 μM, each deoxynucleotide at 50 μM, Pwo buffer at 1× (supplied), and Pwo DNA polymerase (Roche Diagnostics) at 25 units/mL was added to the leaf tissue pellet described above. Thirty cycles of 92 °C for 30 s, 60 °C for 45 s, and 72 °C for 1 min were followed by an additional 15 min at 72 °C. The PCR product was digested with *Eco*RI and *Bam*HI and ligated into the similarly digested pGEM3ZF+ vector (Promega). Clones were sequenced and pJC466 was found to be in frame. Comparison of the deduced amino acid sequence with those held in the GenBank database showed that this was a new isoform of abrin A chain (ATA). It was termed abrin F (UK patent application no. GB0102951.1). A further round of PCR was used to add a six-His tag at the N-terminus and introduce the clone into the expression vector pET12a (Novagen). This clone was termed pJC534.

Creation of Abrin A Chain Variants. pJC534 was used as a template for PCR mutagenesis. The amino acid substitutions K6N, K18T, and K151R were introduced sequentially into the ATA sequence and encoded ATA-0K. The residue changes L32K and T61K were separately introduced to encode ATA-5K. Additionally, the residue changes Q122K and N215K were separately introduced, and subsequently an *Nsi*I/*Bam*HI fragment was subcloned back into the ATA-5K sequence to encode ATA-7K.

Expression and Purification of Abrin F A Chain. Two 500 mL cultures of plasmid-bearing *E. coli* strain C41 (*24*) were grown at 37 °C to an OD_{600nm} of 0.7. Expression was induced with 1 mM IPTG for 18 h at 30 °C. Cells were harvested by centrifugation at 3000*g*, resuspended in 40 mL of 50 mM Tris-HCl, pH 8, and sonicated. Cell debris was removed by centrifugation at 31000*g* for 1 h at 4 °C, and the ATA-containing supernatant was loaded onto a Q-Sepharose (Pharmacia) column (140 mm × 25 mm) which had been preequilibrated in the same buffer. Fractions were collected, and those containing ATA were pooled. NaCl (0.5 M) and

imidazole (20 mM) were added, and the sample was applied to a 5 mL chelating Sepharose fast-flow (Pharmacia) column precharged with Ni^{2+} and equilibrated with 50 mM Tris-HCl, pH 8, 0.5 M NaCl, and 20 mM imidazole. The column was washed with increasing concentrations of imidazole, and His-tagged protein eluted with 500 mM imidazole. Fractions containing pure ATA were pooled and dialyzed against 25 mM Tris-HCl, pH 8, with a stepwise decrease in imidazole concentration to prevent protein precipitation. Glycerol was added to a final concentration of 15% (v/v), and samples were stored at −20 °C.

Production of Abrin B Chain. Abrin (7 mg) was mixed with 6% β-mercaptoethanol in a buffer of 50 mM Tris-HCl, pH 8.0, and 0.1 M lactose overnight at 4 °C. The mixture was loaded onto a 7 mL cibacron-3GA (Sigma) column preequilibrated with 50 mM Tris-HCl, pH 8.0, 0.1 M lactose, and 6% β-mercaptoethanol. The ATA binds to the cibacron, and the flow-through material containing abrin B chain (ATB) was collected. The sample was dialyzed against 25 mM Tris-HCl, pH 8.0, and 0.1 M lactose and then concentrated to 0.6 mL. Dithiothreitol (DTT) was added (1 mM final concentration), and the sample was loaded onto a 17 mm × 280 mm Sephacryl S200 (Pharmacia) column preequilibrated in the same buffer. Fractions were collected, and those containing ATB were pooled. The purified ATB fraction did not contain significant contaminating abrin holotoxin, since it was nontoxic to cells in cytotoxicity assays (performed as described below).

Determination of the Catalytic Activity of RTA Variants. The catalytic activity of RTA variants was determined by assessing their ability to depurinate 26S ribosomal RNA (rRNA) of purified *Saccharomyces cerevisiae* ribosomes. In each 20 μL reaction, a known amount of RTA was incubated with 20 μg of ribosomes in 25 mM Tris-HCl, pH 7.6, 25 mM KCl, and 5 mM $MgCl_2$ for 60 min at 30 °C. Reactions were stopped by addition of 180 μL of Kirby buffer (*25*) and 200 μL of phenol/chloroform (1:1 v/v), and rRNA was recovered by ethanol precipitation. Four micrograms of RTA-treated rRNA was incubated with acetic aniline for 2 min at 60 °C; rRNA was ethanol precipitated, resuspended in TPE (3.6 mM Tris base, 3.0 mM NaH_2PO_4, 0.2 mM EDTA)−60% (v/v) formamide, and heated to 60 °C for 2 min. rRNA fragments were separated on 1.2% (w/v) agarose−50% (v/v) formamide gels and visualized by ethidium bromide staining (*26*).

Determination of Ricin A Chain Protease Stability. RTA (500 ng) was incubated with trypsin (0.5−50 μg/mL) at 37 °C for 15 min in a volume of 20 μL as described previously (*27*). Proteolysis was terminated by boiling the reactions for 5 min in SDS−PAGE sample buffer, and protein fragments were separated by SDS−PAGE and visualized by silver staining.

Reassociation of Ricin A Chains with Ricin B Chain. RTA (50 μg) was mixed with 50 μg of purified RTB (Vector Labs) in a total volume of 1 mL of PBS containing 0.1 M lactose and 2% β-mercaptoethanol. The mixture was dialyzed overnight against 0.1 M lactose in PBS at 4 °C and then against PBS over three nights at 4 °C. Reassociated holotoxin was purified away from free RTA on a 0.5 mL lactose−agarose column as previously described (*28*). The concentration of holotoxin was determined by comparison with RTA standards of known concentration on silver-stained SDS−PAGE gels and quantification using ImageQuant software. ATA and ATB were reassociated in the same way to regenerate abrin holotoxin.

Determination of Holotoxin Interchain Disulfide Bond Stability. Reassociated holotoxin (100 ng) was incubated with increasing concentrations (0.1−10 mM) of dithiothreitol for 30 min at 37 °C. Reactions were quenched by incubation with iodoacetamide (final concentration of 20 mM) for 10 min at 37 °C before being subjected to nonreducing SDS−PAGE and silver staining.

Maintenance of Tissue Culture Cells. Vero cells were grown at 37 °C in Dulbecco's modified Eagle medium (DMEM) supplemented with 5% fetal calf serum (FCS), 2 mM glutamine, 100 units/mL penicillin, and 100 μg/mL streptomycin sulfate in a humidified 5% CO_2 incubator. Chinese hamster ovary cells (E36 and ts20 cells) were grown at the permissive temperature (30.5 °C) in α minimal essential medium supplemented with 10% FCS, glutamine, penicillin, and streptomycin, as stated above for Vero cells, in a humidified 5% CO_2 incubator.

Cytotoxicity Assays. Vero cells were seeded at a concentration of 1.5×10^5 cells/mL into flat-bottomed 96-well plates and grown overnight at 37 °C. Cells were washed with PBS and then overlayed with 100 μL of DMEM containing appropriate concentrations of ricin. After 4 h, the toxin was removed, and the cells were washed twice with PBS before the addition of 1 μCi of [^{35}S]methionine in 50 μL of PBS and incubation for 2 h. Labeled proteins were precipitated by three washes with 5% trichloroacetic acid, followed by two washes with PBS. After addition of 200 μL of Optiphase "SuperMix" scintilation fluid (Wallac), the amount of radioactivity incorporated was determined by scintillation counting in a MicroBeta 1450 Trilux counter. For experiments using *clasto*-lactacystin β-lactone, Vero cells were pretreated at 37 °C for 1 h with 50 μL of DMEM containing the inhibitor at a concentration of 20 μM, and 4 h toxin incubations were also performed in the presence of the inhibitor. CHO E36 and ts20 cells were seeded at a concentration of 6.5×10^5 cells/mL into 96-well plates and grown at the permissive temperature of 30.5 °C for 24 h. After the cells were washed with PBS, they were incubated at the permissive (30.5 °C) or the nonpermissive (40.5 °C) temperature for 1 h before toxin addition. Two hundred microliters of toxin in MEM−α medium was added per well, and the plates were incubated at the appropriate temperature (30.5 or 40.5 °C) for 16 h. Protein synthesis was determined as described above for Vero cells.

Pulse−Chase Analysis of Ribophorin I (RI_{332}) Degradation in Chinese Hamster Ovary Cells. Both parental (E36) and mutant (ts20) cells were seeded at a concentration of 6.5×10^5 cells/dish into 3.5 cm dishes and grown for approximately 24 h before use at 30.5 °C in MEM−α medium supplemented as before. Cells were then washed twice with PBS before the addition of 1 mL of methionine-free media. Cells were then incubated at either 30.5 or 40.5 °C for 1 h. The medium was aspirated, and 1 mL of methionine-free medium containing 40 μCi of [^{35}S]methionine was added (preequilibrated to either 30.5 or 40.5 °C). After a 5 min pulse at 30.5 or 40.5 °C, the medium was removed and replaced with 1 mL of MEM−α, and incubation was continued at the appropriate temperature. At timed intervals the medium was removed, and the cells were washed once with ice-cold PBS.

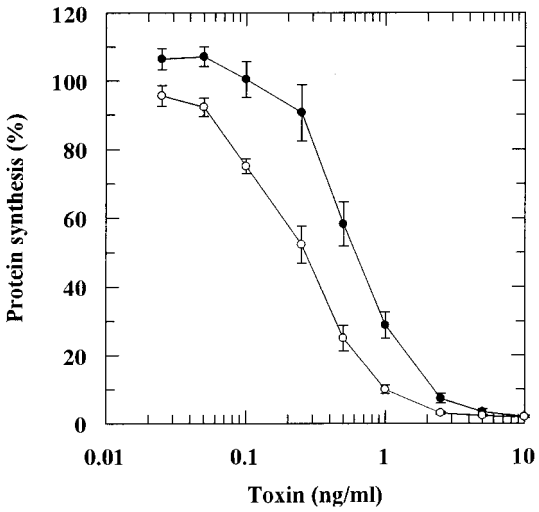

FIGURE 1: Treating Vero cells with a proteasome inhibitor increases their sensitivity to ricin. Cells were incubated with 20 μM *clasto*-lactacystin β-lactone in dimethyl sulfoxide (DMSO) (○) or DMSO only (●) for 1 h at 37 °C prior to the addition of ricin. The inhibitor was present during toxin treatment. Cells were challenged with increasing concentrations of ricin containing wild-type recombinant RTA for 4 h at 37 °C and then given a 2 h pulse with [^{35}S]methionine. The amount of radioactivity incorporated into protein in toxin-treated cells was expressed as a percentage of that incorporated by untreated cells. Error bars represent ±1 standard deviation.

Cells were lysed by the addition of 0.5 mL of lysis buffer [95 mM NaCl, 3 mM EDTA, 2% (w/v) SDS, 25 mM Tris-HCl, pH 7.4, 1 mM DTT, Complete protease inhibitors (Roche Diagnostics, GmbH)], and cell lysates were boiled for 10 min prior to a 1 in 4 dilution with dilution buffer [95 mM NaCl, 3 mM EDTA, 25 mM Tris-HCl, pH 7.4, 1 mM DTT, 0.2% (w/v) SDS, 1.25% (v/v) Triton X-100]. Cell debris was removed by centrifugation, and the supernatants were tumbled with 50 μL of pansorbin for 30 min at 4 °C. Supernatants were transferred to fresh tubes containing 50 μL of protein A−Sepharose and 2.5 μL of polyclonal rabbit anti-ribophorin I antibody (approximately 5 μL for every 10^6 cells) and tumbled overnight at 4 °C. The protein A−Sepharose matrix was washed twice with 1 mL of dilution buffer and twice with 1 mL of PBS and then resuspended in 40 μL of sample buffer [20% (v/v) glycerol, 5% (w/v) SDS, 10 mM Tris-HCl, pH 7.4]. Immunoprecipitated protein was separated by SDS−PAGE and visualized by fluorography.

Circular Dichroism. Far-UV CD spectra were recorded using a Jasco J-715 spectropolarimeter attached to a PTC-348 Peltier-heated cell holder. Spectra were accumulated from 190 to 250 nm using a 1 mm path length cuvette and RTA at a concentration of 6 μM in 5 mM sodium phosphate, pH 6.5. For temperature ramping experiments the temperature was increased at a rate of 1 °C per minute.

RESULTS

RTA Entering the Cytosol Is Degraded by Proteasomes. If a significant proportion of the RTA that enters the cytosol from the ER undergoes proteasomal degradation, then treating Vero cells with the proteasome inhibitor *clasto*-lactacystin β-lactone might be expected to increase the cytotoxic potency of the ricin holotoxin. As shown in Figure 1, and in keeping with an earlier report (*5*), Vero cells [and other cell lines (not shown)] treated with the inhibitor were approximately 3-fold more sensitive to ricin than their untreated counterparts. The fact that ricin is potently cytotoxic to mammalian cells in the absence of proteasomal inhibition clearly indicates that a proportion of RTA entering the cytosol from the ER avoids immediate degradation.

Table 1: Summary of the in Vitro Catalytic Activities of the RTA Variants

RTA protein	IC_{50} (pg/μL)[a]	relative *N*-glycosidase activity
0K	55	1.2
wild type (2K)	65	1.0
4K1	90	0.7
4K2	13	5.0
6K	32	2.0
4R	50	1.3

[a] RTA concentration required to obtain 50% of the maximum observed depurination. Standard errors were <10%.

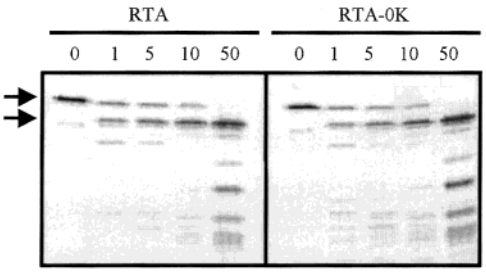

FIGURE 2: Sensitivity of recombinant wild-type RTA and RTA-0K to trypsin. Samples (500 ng) of each protein were incubated with increasing concentrations of trypsin for 15 min at 37 °C. Samples were then boiled in reducing buffer, resolved by SDS−PAGE, and silver stained. The upper arrow indicates the position of RTA and the lower arrow that of trypsin.

Native RTA Is Not an Effective Substrate for Ubiquitination. The observation that all toxins known to enter the cytosol from the ER have an extremely low lysine content may point to an evolutionary strategy for escaping ubiquitin conjugation (*22*). If correct, this might indicate that the two lysyl residues naturally present in RTA have been retained because they are not effective substrates for ubiquitination. To test this, lysyl residues at positions 4 and 239 were mutagenised to arginyl residues. The variant protein, designated RTA-0K, was expressed in *E. coli* and purified to homogeneity as judged by SDS−polyacrylamide gel electrophoresis (data not shown). The RTA-0K variant was indistinguishable from native RTA in terms of its catalytic activity (Table 1), its ability to reassociate with (and, when titrated with thiol reducing agents, dissociate from) RTB (data not shown), and its resistance to trypsin treatment (Figure 2). It is well established that native RTA is resistant to proteases such as trypsin (*23*) and proteinase K (*29*), but when deliberately unfolded or destabilized by certain point mutations, it becomes sensitive (for example, see ref *29*). The data shown in Figure 2 suggest that RTA-0K has the native, protease-resistant structure. In keeping with this, the cytotoxicity of ricin obtained by reassociating RTA-0K with RTB was identical to that of ricin reconstituted from wild-type RTA and RTB (Table 2). The fact that removal of the two endogenous lysines did not increase toxin potency suggests that these residues are not targets for ubiquitination

Table 2: Summary of the IC_{50} Values of the Ricin Variants toward Vero Cells

ricin protein	IC_{50} (ng/mL)[a]	relative cytotoxicity (%)
0K	0.6	100
wild type (2K)	0.6	100
4K1	15.0	4
4K2	32.0	2
6K	50.0	1
4R	2.3	26

[a] Standard errors were <10%.

Table 3: Summary of the IC_{50} Values of Ricin Variants in the Absence and Presence of the Proteasomal Inhibitor *clasto*-Lactacystin β-Lactone

ricin protein	IC_{50} (ng/mL)[a]	IC_{50} (ng/mL) + β-lactone	increase in cytotoxicity
0K	0.6	0.4	1.5-fold
wild type (2K)	0.6	0.3	2.0-fold
4K1	14.0	1.5	9.3-fold
4K2	15.0	0.6	25.0-fold
6K	64.0	1.0	64.0-fold
4R	2.7	1.2	2.3-fold

[a] Standard errors were <10%.

enzymes. Treating cells with *clasto*-lactacystin β-lactone sensitized them to ricin containing RTA-0K ~1.5-fold (Table 3), indicating that proteasomal degradation of a proportion of RTA-0K occurred. This supports the contention that during normal cell entry native RTA is largely degraded by the proteasome, possibly in an ubiquitin-independent manner.

Increasing the Lysine Content of RTA. We rationalized that if the low lysine content of RTA permits degradation avoidance, then the introduction of additional lysyl residues might increase predisposition for ubiquitination and the consequent level of proteasomal degradation. To introduce lysyl residues in positions that would not compromise other properties of the resulting protein, the sites selected were based on a detailed structural comparison of RTA with a closely related protein that does not enter the cytosol from the ER lumen. Pokeweed antiviral protein (PAP) is a single-chain member of the ribosome-inactivating protein family that is structurally homologous to RTA (*30*). Unlike ricin, PAP does not have a cell-binding B chain and is therefore unable to enter cells with the same efficiency. In marked contrast to RTA, PAP contains a total of 20 lysyl residues. By superimposing the structures of PAP and RTA (*31*) (Figure 3), it is evident that the surface-exposed Val38, Glu67, Asn132, and Ser228 of RTA could be replaced by lysyl residues, since these occur in the equivalent positions in PAP. Accordingly, the RTA variant designated RTA-6K was prepared along with two intermediates, in which just two additional lysine residues were introduced by replacing either Val38 and Glu67 (RTA-4K1) or Asn132 and Ser228 (RTA-4K2), respectively. None of the introduced lysyl residues were positioned to interface with RTB.

Properties of RTA Lysine Variants. RTA-6K, RTA-4K-1, and RTA-4K-2 were purified to homogeneity from *E. coli* expression cultures (data not shown). We confirmed that the introduced lysyl residues did not affect the stability of these proteins but will only describe data demonstrating this for RTA-6K. RTA-6K and RTA were very similar in their catalytic activities (Table 1) and their sensitivities to trypsin

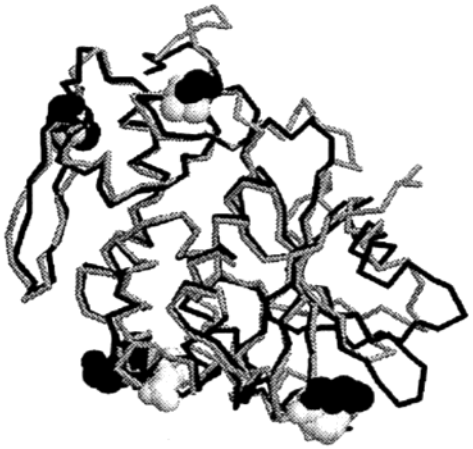

FIGURE 3: Superimposition of the α-C backbone structures of RTA (black) and pokeweed antiviral protein (PAP) (gray). Four of the lysyl residues in PAP and the corresponding residues in RTA that were changed to lysines are shown space-filled.

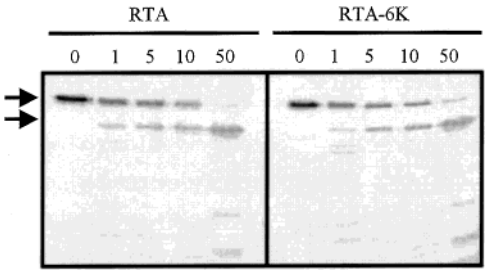

FIGURE 4: Sensitivity of recombinant wild-type RTA and RTA-6K to trypsin. Samples (500 ng) of each protein were incubated with increasing concentrations of trypsin for 15 min at 37 °C. Samples were then boiled in reducing buffer, resolved by SDS−PAGE, and silver stained. The upper arrow indicates the position of RTA and the lower arrow that of trypsin.

digestion (Figure 4). As in the case of RTA-0K, RTA-6K readily formed stable holotoxin upon reassociation with RTB (data not shown). The far-UV CD spectrum and intrinsic protein fluorescence spectrum of RTA were unchanged for all of the lysine variants described, suggesting that the introduced substitutions did not cause any significant structural changes (data not shown). We were concerned that the introduced lysyl residues might have destabilized the protein such that any observed decrease in apparent cytotoxicity might have resulted from decreased stability rather than enhanced proteasomal degradation. Accordingly, we compared the temperature-induced unfolding of RTA with RTA-6K as determined by far-UV circular dichroism. In fact, the introduced lysyl residues had a significant stabilizing effect on the protein, conferring a 7 °C increase in thermal stability (Figure 5). A possible explanation for this increase in thermal stability could be due to the replacement of a surface-exposed hydrophobic residue (V38) with a charged hydrophilic group. We conclude that the introduction of additional lysyl residues into RTA, based on their relative positions in PAP, was without deleterious effect on the stability or catalytic properties of the protein.

Lysine-Rich RTA Is More Susceptible to Proteasomal Degradation. When the cytotoxicities of ricin containing RTA-6K and ricin containing wild-type RTA were compared, the former was found to be 2 orders of magnitude less cytotoxic than the native toxin to Vero cells (Figure 6). The

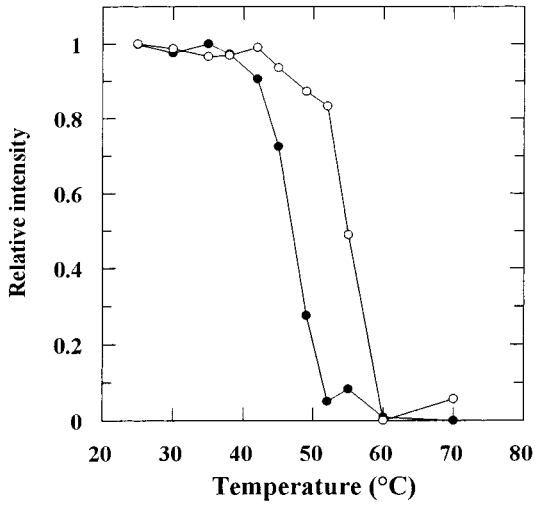

FIGURE 5: Introduction of extra lysyl residues increases thermal stability of RTA. Changes in the far-UV CD of recombinant wild-type RTA (●) and RTA-6K (○) (6 μM) were monitored continuously at 208 nm, and the temperature was increased from 25 to 70 °C at 1 °C per minute. Relative intensity was calculated as $1 - [(\theta_n - \theta_t)/(\theta_n - \theta_u)]$, where θ_n, θ_u, and θ_t are the molecular ellipticities (208 nm) of the native protein, fully thermally unfolded protein, and protein at temperature t °C, respectively.

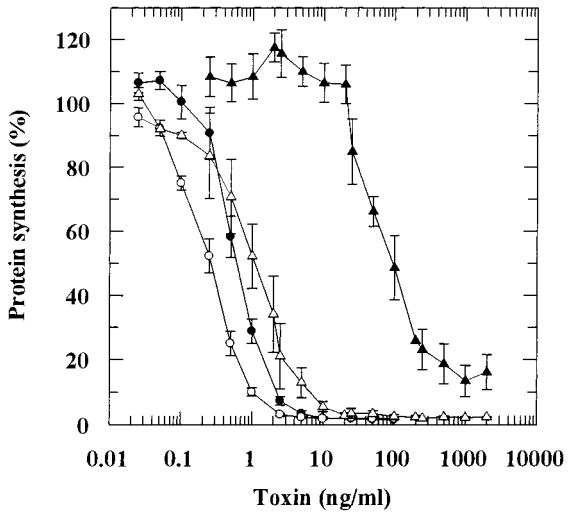

FIGURE 6: Extra lysyl residues introduced into RTA predispose it to proteasomal degradation. Vero cells were incubated with either 20 μM *clasto*-lactacystin β-lactone or its solvent DMSO for 1 h prior to the addition of toxin. The inhibitor was present during toxin treatment. Cells were challenged with increasing concentrations of holotoxin for 4 h at 37 °C before a 2 h pulse with [^{35}S]methionine. Protein synthesis by toxin-treated cells was calculated as a percentage of that determined for untreated cells. Symbols: (●) ricin containing wild-type RTA; (○) ricin containing wild-type RTA in the presence of inhibitor; (▲) ricin containing RTA-6K; (△) ricin containing RTA-6K in the presence of inhibitor. Error bars represent ±1 standard deviation.

IC_{50} (the concentration of toxin that caused a 50% reduction in protein biosynthetic capacity) of ricin containing RTA-6K was 50 ng/mL compared to 0.6 ng/mL for native ricin (Table 2). The reduced cytotoxicity of ricin containing RTA-6K resulted from enhanced proteasomal degradation, since treating the cells with the specific proteasome inhibitor *clasto*-lactacystin β-lactone restored potency close to the level seen with native toxin (Figure 6).

That the reduced cytotoxicity did not simply result from the addition of positive charges was demonstrated using another RTA variant in which the same four residues were changed to arginine (RTA + 4R). The catalytic activity (Table 1), stability, and the extent and stability of reassociation with RTB were identical when RTA + 4R was compared with native RTA (data not shown). The cytotoxicity of ricin containing RTA + 4R was only marginally lower than that of the native holotoxin but clearly distinct from that of RTA-6K (Table 2). The cytotoxicities of ricin containing either RTA-4K-1 or RTA-4K-2 were intermediate between toxin containing either RTA or RTA-6K, being reduced 25- and 53-fold, respectively, when compared with native holotoxin (Table 2).

Active Ubiquitination Is Required for the Downregulation of RTA-6K. The ubiquitin/proteasome pathway has been shown to mediate the degradation of a truncated form of ribophorin I (RI_{332}; *20*). To indirectly test whether an active ubiquitination system affects ricin cytotoxicity, CHO cells stably expressing RI_{332} (designated CHO-E36) were selected as a parental cell line. CHO-ts20 cells, which express a thermolabile ubiquitin-activating enzyme E1 (*32*, *33*) and which also express RI_{332}, were chosen as the ubiquitination-defective cell line. At the nonpermissive temperature of 40.5 °C, this mutation dramatically reduces (but does not eliminate) ubiquitin-mediated proteasomal degradation (*20*). Here we confirmed that RI_{332} is rapidly degraded at the restrictive temperature in CHO-E36 cells, whereas it is stabilized in CHO-ts20 cells (Figure 7a). Similar immunoprecipitations to track the kinetics of RTA degradation are not possible owing to the tiny amounts of RTA that actually reach the ER lumen of intoxicated cells. However, since the extent of ubiquitin-mediated proteasomal degradation can be monitored by the toxic effect of protein escaping this fate, cytotoxicity experiments were performed. At the permissive temperature (30 °C), where ubiquitination is unaffected in CHO-ts20 cells, ricin-6K had no significant cytotoxic effect on either CHO-E36 or CHO-ts20. In contrast, when the temperature was increased to the nonpermissive temperature (40.5 °C), where ubiquitination is blocked in CHO-ts20 cells but unaffected in CHO-E36 cells while ricin-6K remained nontoxic to CHO-E36 cells, it now possessed cytotoxicity toward CHO-ts20 cells (Figure 7b). At the nonpermissive temperature when ubiqitination is effectively blocked, ricin-6K had an IC_{50} of ~40 ng/mL, at least 50-fold more toxic than at the permissive temperature. Native ricin was approximately equally toxic to both CHO-E36 and CHO-ts20 cells at both the permissive and nonpermissive temperatures, although there was almost an order of magnitude increase in toxicity for both cell types at 40.5 °C as compared to 30 °C. This lack of effect of the ubiquitination mutation on ricin toxicity was consistent with the earlier contention that ricin is normally partially degraded in a ubiquitin-independent manner.

The Low Lysine Content of Abrin A Chain Also Precludes Extensive Proteasomal Degradation. To broaden the evidence that the low lysine makeup of toxins translocating from the ER is physiologically relevant, we have applied the same experimental approach to study the fate of abrin A chain in cells. Abrin is a heterodimeric plant toxin that is functionally related to ricin, and its A chain (ATA) contains three lysyl residues. DNA encoding ATA (*34*) was therefore mutagenized to change the three lysine codons into the equivalent codons of ricin A chain (Lys6-Asn, Lys18-Thr, and Lys151-

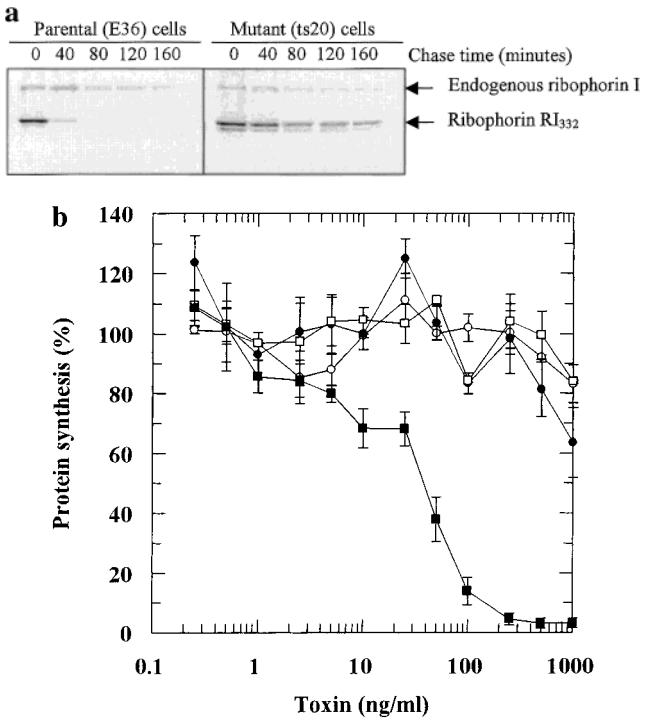

FIGURE 7: Sensitivity of E36 and ts20 cells to ricin containing RTA-6K. (a) Degradation of truncated ribophorin 1 (RI_{332}) in parental and mutant CHO cells. Cells were preincubated at the nonpermissive temperature (40.5 °C) for 1 h before being labeled for 5 min with [^{35}S]methionine and then chased for the times indicated in methionine-free media. Cells were then lysed and the lysates immunoprecipitated for ribophorin 1. Samples were analyzed by SDS−PAGE and autoradiography. (b) Cells were incubated at the permissive temperature (30.5 °C) or the nonpermissive temperature (40.5 °C) for 1 h. Cells were then challenged with increasing concentrations of ricin containing RTA-6K for 16 h at either 30.5 or 40.5 °C before receiving a 2 h pulse of [^{35}S]-methionine. Protein synthesis by toxin-treated cells was calculated as a percentage of that determined for untreated cells. Symbols: (○) E36 cells at 30.5 °C; (●) ts20 cells at 30.5 °C; (□) E36 cells at 40.5 °C; (■) ts20 cells at 40.5 °C. Error bars represent ±1 standard deviation.

Arg) in order to generate a protein product designated ATA-0K. Additionally, ATA was made with two or four supplementary lysyl residues [ATA-5K (Leu32-Lys and Thr61-Lys) and ATA-7K (Leu32-Lys, Thr61-Lys, Gln122-Lys, and Asn215-Lys), respectively] at positions equivalent to those described in the generation of RTA-4K-1 and RTA-6K. The ATA variants were purified to homogeneity from *E. coli* expression cultures as determinmed by SDS−PAGE (data not shown). As in the case of RTA, the ATA variants were indistinguishable from native ATA in terms of their catalytic activity, stability, and association/disassociation with ATB (data not shown). The variant ATAs were reassociated with purified ATB, and the holotoxin potencies were monitored when applied to Vero cells. We found that the cytotoxicity of abrin containing ATA-0K was identical to that of the native toxin (Table 4). The cytotoxicity of abrin containing ATA-7K was markedly reduced but could be restored to a significant extent by pretreating cells with *clasto*-lactacystin -β-lactone (Figure 8 and Table 4), while the cytotoxicity of abrin containing ATA-5K was intermediate in potency (Table 4).

Table 4: Effect of *clasto*-Lactacystin β-Lactone on the Cytotoxicity of Substituted Abrin Variants

abrin variant	IC_{50} (ng/mL)[a]	IC_{50} (ng/mL) + β-lactone	increase in cytotoxicity
0K	2.0	1.3	1.5-fold
wild type (3K)	3.5	2.0	1.8-fold
5K	10.0	0.8	12.5-fold
7K	>1000.0	20.0	>50.0-fold

[a] Standard errors were <10%.

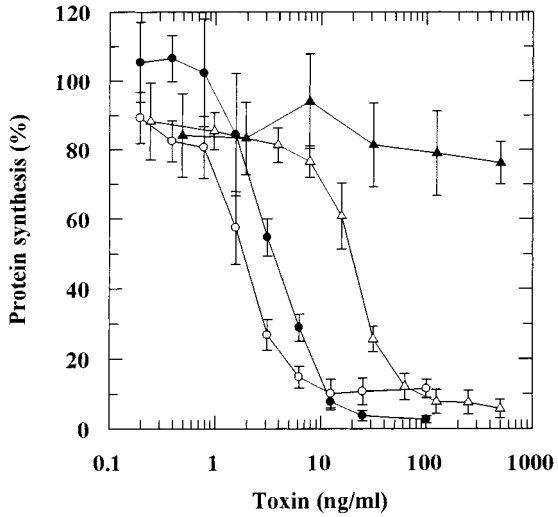

FIGURE 8: Extra lysyl residues introduced into ATA predispose it to proteasomal degradation. Vero cells were incubated with either 20 μM *clasto*-lactacystin β-lactone or its solvent DMSO for 1 h prior to the addition of toxin. The inhibitor was present during toxin treatment. Cells were challenged with increasing concentrations of toxin for 4 h at 37 °C before a 2 h pulse with [^{35}S]methionine. Protein synthesis by toxin-treated cells was calculated as a percentage of that determined for untreated cells. Symbols: (●) abrin F containing wild-type ATA; (○) abrin F containing wild-type ATA in the presence of inhibitor; (▲) abrin F containing ATA-7K; (△) abrin F containing ATA-7K in the presence of inhibitor. Error bars represent ±1 standard deviation.

DISCUSSION

Ricin is one of several potent toxins able to undergo retrograde transport to the ER of mammalian cells. Other examples include the plant protein abrin and the bacterial proteins cholera toxin, pertussis toxin, *Pseudomonas* exotoxin A, Shiga toxin, and *E. coli* Shiga-like toxin 1 (*35*). To understand how toxins might accomplish the final transport step across the ER membrane, it may be pertinent to draw parallels with endogenous proteins that also undergo such reverse membrane translocation. The ER is the site where newly synthesized proteins normally fold into their native conformation, assisted by resident ER chaperones, and, if appropriate, assemble into oligomers (*36*−*38*). Once the native conformation has been achieved, proteins destined for post-ER locations exit the ER as cargo packaged into ER-to-Golgi transport vesicles (*39*). Proteins that fail to fold correctly, or unassembled orphan subunits of oligomeric proteins, do not leave the ER in transport vesicles. Rather than simply accumulating in the ER lumen, however, such aberrant proteins are eliminated by proteolytic degradation as part of a stringent ER quality control system known as ER-associated degradation (ERAD) (*10*, *12*). This entails their perception as misfolded molecules (*40*−*42*) with

subsequent export to the cytosol followed by proteasomal degradation. ERAD substrates are retrotranslocated across the ER membrane via the Sec61p translocons (*8*, *9*, *12*) that are also responsible for the import of nascent or newly synthesized proteins into the ER (*43*). Once translocated, these proteins are usually (*44*), but not always (*45*), predisposed for proteolytic destruction by ubiquitination: the attachment of multiple molecules of the 76-residue protein to the ϵ-amino group of appropriate lysyl residues (*19*). Attachment of ubiquitin to the amino terminus may also occur (*18*). Such modification ensures efficient targeting to the proteasomal cap structure that recognizes and unfolds the protein in readiness for its entry into the proteasomal core for degradation (*46*).

It has been proposed that catalytic subunits of toxins arriving in the ER lumen can masquerade as ERAD substrates (*3*, *47*). Indeed, experimental evidence has been presented to show that RTA introduced into the ER lumen of tobacco protoplasts (*48*) and cholera toxin A fragment introduced into ER microsomes (*7*), use the ERAD pathway to translocate to the cytosol. Consistent with this, it has also been shown that RTA export from mammalian ER and cholera toxin export from microsomes in vitro utilized Sec61p translocons (*5*, *7*). However, it remains unclear how RTA might become an unfolded/misfolded candidate for ERAD, though recent work with cholera toxin revealed a role for protein disulfide isomerase as an unfoldase (*49*). Whatever the trigger, masquerading as ERAD substrates to accomplish transport across the ER membrane poses an obvious problem for toxin polypeptides in that such translocation is usually tightly coupled to processes on the trans side of the membrane. These include peptide:*N*-glycanse-mediated deglycosylation (*12*, *50*), ubiquitination (*20*), and proteasomal degradation (*21*). To exert a physiological effect, it is clear that at least a proportion of the exported toxin must escape this sequential processing. The finding here and elsewhere (*5*) that treating cells with a specific proteasome inhibitor causes an ~3-fold increase in the cytotoxic potency of ricin indicates that a significant proportion of RTA entering the cytosol normally becomes degraded by proteasomes. Alternatively, some other cellular component that mediates RTA degradation in the cytosol is itself subject to proteasomal degradation. Regardless of whether the proteasome is directly or indirectly responsible for RTA degradation, the data suggest that toxin degradation is at least partially reduced when proteasomal activity is inhibited (Figure 1). Nevertheless, the fact that toxin potency remains high in the absence of such inhibitors reveals that a lethal dose of translocated toxin always evades an encounter with this degradation machinery (Figures 1 and 6).

The question we have addressed in the present study relates to how this fraction of toxin in the cytosol might avoid proteasomal proteolysis. Degradation of ERAD substrates is usually facilitated by the conjugation of ubiquitin to lysyl residues once the proteins are delivered into the cytosolic milieu (see ref *14* for a review). However, it has been noted that lysyl residues are very uncommon in the A polypeptides of all the toxins known to translocate across the ER membrane (*22*). For example, like RTA, cholera toxin A and Shiga-like toxin 1 A fragments also contain two lysyl residues, *Pseudomons* exotoxin A has only three, *E. coli* heat-labile enterotoxin has one, and pertussis toxin is completely

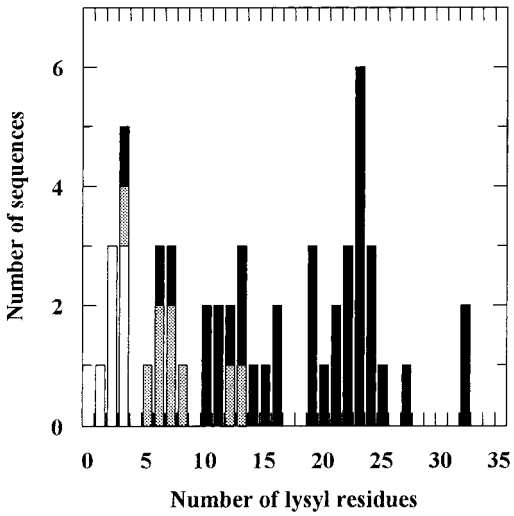

FIGURE 9: Lysine content of ribosome-inactivating proteins: open bars, the A chains of 7 cytotoxic type 2 RIPs; gray bars, the A chains of 9 nontoxic type 2 RIPs; black bars, 36 type 1 RIPs.

devioid of lysyl residues. In contrast, other toxins that enter the cytosol from endosomes away from the immediate vicinity of the ubiquitin/proteasome machinery have a more typical lysine content: diphtheria toxin A fragment, for example, contains 16 lysyl residues. The hypothesis that the low lysine makeup of toxins that retrotranslocate from the ER is an important factor in degradation avoidance correlates well with the occurrence of lysyl residues, not only among the bacterial toxins referred to above but also within the plant ribosome-inactivating protein (RIP) family of structurally related proteins. RIPs which exhibit potent cytotoxicity to mammalian cells as typified by ricin and abrin are classified as type 2 RIPs. There is also a subgroup of type 2 RIPs, exemplified by nigrin (*51*) and ebulin (*52*), which are relatively nontoxic to mammalian cells even though their A chains are as effective as the A chains of ricin and abrin in catalyzing 28S rRNA depurination in vitro. The most common RIPs are type 1 RIPs such as PAP and gelonin that lack a cell-binding B chain and are thus not cytotoxic. Comparing the primary sequences of the different type 1 RIPs and the A chains of type 2 RIPs reveals that the A chains of the seven toxic type 2 RIPs contain an average of 2.3 ± 0.8 lysyl residues per polypeptide. By contrast the A chains of nine nontoxic type 2 RIPs contain an average of 7.4 ± 3.2 (this may partly explain their poor cytotoxicity if they are indeed predisposed to ubiquitination/proteasomal degradation). The 36 type 1 RIPs that do not normally enter cells after endocytosis to the mammalian cell ER contain an average of 18.6 ± 6.9 lysyl residues (Figure 9).

Removal of the two endogenous lysyl residues from RTA, or the three from ATA, did not have any discernible effect on potency as judged by protein synthesis inhibition in comparison with native toxin. Though indirect, this lack of effect would suggest that attachment of ubiquitin to the naturally occurring lysyl residues does not normally occur during cell intoxication. It also supports the notion that toxin degradation in the cytosol is not ubiquitin-mediated. There are precedents for ubiquitin-independent proteasomal degradation in the case of ornithine decarboxylase (*15*) and the cyclin-dependent kinase inhibitor $p21^{Cip1}$ (*16*) in mammalian cells and possibly pro-α factor in yeast (*17*). However, even

after removal of all lysyl residues, a fraction of RTA and ATA may still be targeted for proteasomal degradation via N-terminal ubiquitination (*18*).

In contrast, the introduction of four additional lysyl residues into RTA (RTA-6K) and ATA (ATA-7K) predisposed the ER-exported toxins for ubiquitination and consequent targeting to the proteasome. This occurred even though the lysine-rich RTA exhibited greater thermal stability than wild-type RTA (Figure 5). The observation that a CHO cell line with a defect in the ubiquitin-activating enzyme E1 (*31*) was less sensitive to intoxication by ricin containing RTA-6K than were the parental CHO-E36 cells (Figure 7b) strongly implicates the lysyl residues of RTA-6K as targets for ubiquitination. The consequences of altering the lysine composition of RTA and ATA, and the correlation between low lysine content and the cell entry characteristics of the toxin, clearly suggest that a dearth of lysine residues attenuates what might otherwise be a most effective cellular process for removing, and thereby disarming, this class of toxin in the cytosol.

REFERENCES

1. Lord, J. M., Roberts, L. M., and Robertus, J. D. (1994) *FASEB J. 8*, 201−208.
2. Endo, Y., Mitsui, K., Motiguki, M., and Tsurugi, K. (1987) *J. Biol. Chem. 262*, 5908−5912.
3. Rapak, A., Falnes, P. O., and Olsnes, S. (1997) *Proc. Natl. Acad. Sci. U.S.A. 94*, 3783−3788.
4. Lord, J. M., and Roberts, L. M. (1998) *J. Cell Biol. 140*, 733−736.
5. Wesche, J., Rapak, A., and Olsnes, S. (1999) *J Biol. Chem. 274*, 34443−34449.
6. Falnes, P. O., and Sandvig, K. (2000) *Curr. Opin. Cell Biol. 12*, 406−413.
7. Schmidz, A., Herrgen, H., Winkeler, A., and Herzog, V. (2000) *J. Cell Biol. 148*, 1203−1212.
8. Pilon, M., Schekman, R., and Römisch, K. (1997) *EMBO J. 16*, 4540−4548.
9. Plemper, R. K., Böhmler, S., Bordallo, J., Sommer, T., and Wolf, D. H. (1997) *Nature 388*, 891−895.
10. Brodsky, J. L., and McCracken, A. A. (1997) *Trends Cell Biol. 7*, 151−156.
11. Hampton, R. Y. (1998) *Curr. Opin. Lipidol. 9*, 93−97.
12. Wiertz, E. J., Tortorella, D., Bogyo, M., Yu, J., Mothes, W., Jones, T. R., Rapoport, T. A., and Ploegh, H. L. (1996) *Nature 388*, 432−438.
13. Kopito, R. R. (1997) *Cell 88*, 427−430.
14. Bonafacino, J. S., and Weissman, A. M. (1998) *Annu. Rev. Cell Dev. Biol. 14*, 19−57.
15. Elias, S., Bercovich, B., Kahana, C., Coffino, P., Fischer, M., Hilt, W., Wolf, D. H., and Ciechanover, A. (1995) *Eur. J. Biochem. 229*, 276−285.
16. Sheaff, R. J., Singer, J. D., Swanger, J., Smitherman, M., Roberts, J. M., and Clurman, B. E. (2000) *Mol. Cell 5*, 403−410.
17. Werner, E. D., Brodsky, J. L., and McCracken, A. A. (1996) *Proc. Natl. Acad. Sci. U.S.A. 93*, 13797−13801.
18. Breitschopf, K., Bengal, E., Ziv, T., Admon, A., and Ciechanover, A. (1998) *EMBO J. 17*, 5964−5597.
19. Hershko, A., and Ciechanover, A. (1998) *Annu. Rev. Biochem. 67*, 452−479.
20. de Virgilio, M., Weninger, H., and Ivessa, E. (1998) *J. Biol. Chem. 273*, 9734−9743.
21. Chillaron, J., and Haas, I. G. (2000) *Mol. Biol. Cell 11*, 217−226.
22. Hazes, B., and Read, R. J. (1997) *Biochemistry 36*, 11051−11054.
23. Ready, M. P., Kim, Y., and Robertus, J. D. (1991) *Proteins 10*, 270−278.
24. Miroux, B., and Walker, J. E. (1996) *J. Mol. Biol. 260*, 289−298.
25. Kirby, K. S. (1968) *Methods Enzymol. 12B*, 87−100.
26. May, M. J., Hartley, M. R., Roberts, L. M., Krieg, P. A., Osborn, R. W., and Lord, J. M. (1989) *EMBO J. 8*, 301−308.
27. Simpson, J. C., Lord, J. M., and Roberts, L. M. (1995) *Eur. J. Biochem. 232*, 458−463.
28. Wales, R., Richardson, P. T., Roberts, L. M., Woodland, H. R., and Lord, J. M. (1991) *J. Biol. Chem. 266*, 19172−19179.
29. Walker, D., Chaddock, A. M., Chaddock, J. A., Roberts, L. M., Lord, J. M., and Robinson, C. (1996) *J. Biol. Chem. 271*, 4082−4085.
30. Monzingo, A. F., Collins, E. J., Ernst, S. R., Irvin, J. D., and Robertus, J. D. (1993) *J. Mol. Biol. 233*, 705−715.
31. Katzin, B. J., Collins, E. J., and Robertus, J. D. (1991) *Proteins 10*, 251−259.
32. Kulka, R. G., Raboy, B., Schuster, R., Parag, H., Diamond, G., Ciechanover, A., and Marcus, M. (1988) *J. Biol. Chem. 263*, 15726−15731.
33. Handley-Gearhart, P. M., Trausch-Azar, J. S., Ciechanover, A., and Schwartz, A. L. (1994) *Biochem. J. 304*, 1015−1020.
34. UK Patent Application No. GB0102951.1.
35. Lord, J. M., Smith, D. C., and Roberts, L. M. (1999) *Cell. Microbiol. 1*, 85−91.
36. Hammond, C., and Helenius, A. (1995) *Curr. Opin. Cell Biol. 7*, 523−529.
37. Ellgaard, L., Molinari, M., and Helenius, A. (1999) *Science 286*, 1882−1888.
38. Zapun, A., Jakob, C. A., Thomas, D. Y., and Bergeron, J. J. M. (1999) *Struct. Folding Des. 7*, R173.
39. Rothman, J. E. (1994) *Nature 372*, 611−614.
40. Jakob, C. A., Burda, P., Roth, J., and Aebi, M. (1999) *J. Cell Biol. 142*, 1223−1233.
41. Wilson, C. M., Farmery, M. R., and Bulleid, N. J. (2000) *J. Biol. Chem. 275*, 21224−21232.
42. Knittler, M. R., Dirks, S., and Haas, I. G. (1995) *Proc. Natl. Acad. Sci. U.S.A. 92*, 1764−1768.
43. Rapoport, T. A., Jungnickel, B., and Kutay, U. (1996) *Annu. Rev. Biochem. 65*, 271−303.
44. Ciechanover, A. (1994) *Cell 79*, 13−21.
45. Verma, R., and Deshaies, R. J. (2000) *Cell 101*, 341−344.
46. Smith, S. E., Koegl, M., and Jentsch, S. (1996) *Biol. Chem. 377*, 437−446.
47. Lord, J. M. (1996) *Curr. Biol. 6*, 1067−1069.
48. Frigerio, L., Vitale, A., Lord, J. M., Ceriotti, A., and Roberts, L. M. (1998) *J. Biol. Chem. 273*, 14194−14199.
49. Tsai, B., Rodighiero, C., Lencer, W. I., and Rapoport, T. A. (2001) *Cell 104*, 937−948.
50. Huppa, J. B., and Ploegh, H. L. (1997) *Immunity 7*, 113−122.
51. Girbes, T., Citores, L., Ferreras, J. M., Rojo, M. A., Iglesias, R., Munoz, R., Arias, F. J., Calonge, M., Garcia, J. R., and Mendez, E. (1993) *Plant Mol. Biol. 22*, 1181−1186.
52. Girbes, T., Citores, L., Iglesias, R., Ferreras, J. M., Munoz, R., Rojo, M. A., Arias, F. J., Garcia, J. R., Mendez, E., and Calonge, M. (1993) *J. Biol. Chem. 268*, 18195−18199.

BI011580V